New Physics searches with muons: theoretical review *

Andrzej Czarnecki[1)] Robert Szafron[1)]

[1]Department of Physics, University of Alberta, Edmonton, Alberta, Canada T6G 2E1

Abstract: We summarize current issues related to New Physics searches with muons. We focus on the ratio of magnetic moments of the muon and the proton, needed for the muon g_μ–2 determination; on using the bound-electron $g-2$ to help independently check the persisting discrepancy between the measured $g_\mu-2$ and the Standard Model; and on the bound-muon decay as a background for the muon-electron conversion.

Key words: muon anomalous magnetic moment, new physics searches, muon-electron conversion

PACS: 13.35.Bv, 36.10.Ee

1 Introduction

Muon is a powerful probe of New Physics thanks to its long lifetime and a relatively large mass [1, 2]. It can be produced abundantly, so that even its very rare decays can be searched for [3].

There is a persistent discrepancy [4] between the measured value of the muon anomalous magnetic moment $g-2$ [5] and the Standard Model prediction. A recent summary of this puzzle can be found in [6]. On the theory side, the hadronic contribution remains the topic of very active research. Both the vacuum polarization and hadronic light-by-light [7, 8] effects are being scrutinized. New experiments are being prepared in Fermilab [9] and J-PARC [10] to remeasure the muon $g-2$. The Brookhaven experiment E821 found

$$a_\mu = \frac{g_\mu - 2}{2} = 116\,592\,080(63)\cdot 10^{-11}, \qquad (1)$$

achieving a precision of 0.54 part per million (ppm) and improving the result of earlier experiments at CERN by a factor of 14 [11]. The new efforts hope to reach 0.14 ppm [9] or better.

In parallel, a new measurement of the muonium hyperfine splitting (HFS) is being prepared at J-PARC [12]. It is necessary in order to extract the muon g–2 from the measurements of the anomalous precession of the muon spin [9, 10]. We review this topic in Section **2**.

Electron's g–2 has been measured with a much higher precision than that of the muon [13]. However, since the electron is about 207 times lighter than the muon, it is 43 000 times less sensitive to the New Physics. Measurements of the electron $g-2$, both free and bound, are presently used to precisely determine the fundamental constants m_e and α. However, if α can be determined independently, the precision of the electron g–2 measurements may eventually allow us to probe New Physics, in a manner competitive to the muon.

At present, the best determination of α independent of the electron $g-2$ relies on a combination of the Rydberg constant [14] with the ratio of the electron mass to the Planck constant [15]. However, α enters the properties of many other systems that involve electromagnetic interactions and can be determined from any such system, provided it can be precisely characterized both experimentally and theoretically [16]. A recently proposed approach involves the g factor of a bound electron [17]. We describe some related developments in Section **3**.

The most important current search for New Physics with muons involves the lepton-flavor violating (LFV) decay $\mu \to e\gamma$ [18]. Other LFV processes will be searched for by expriments now under construction: $\mu \to eee$ [19] and the muon-electron conversion near a nucleus. For the latter, there are three new experimental efforts, DeeMe [20], Mu2e [21], and COMET [22]. In Section **4** we discuss the recent progress in the description of the decay of a muon bound in at atom. High-energy electrons produced in this decay are a background for the conversion searches.

2 Magnetic moment of a bound muon

Muonium is a bound state of an electron and an antimuon, both spin 1/2 particles. The lowest energy state is a total spin 0 singlet. The difference of its energy with the spin 1 triplet is called the hyperfine splitting, ΔE_{HFS}.

Received 14 Sep. 2014

∗ Supported by the Natural Sciences and Engineering Research Council of Canada (NSERC).

1) E-mail: andrzejc@ualberta.ca

2) E-mail: szafron@ualberta.ca

2.1 Extraction of the muon to proton magnetic moment ratio

We consider the electron and the muon in a magnetic field oriented along the z direction, $\vec{B}=(0,0,B)$. The interaction Hamiltonian is

$$H=-(\vec{\mu}_e+\vec{\mu}_\mu)\cdot\vec{B}+\Delta E_{\mathrm{HFS}}\vec{I}\cdot\vec{J}, \tag{2}$$

where $\vec{I}$ and $\vec{J}$ are muon and electron spins for which we have

$$\begin{aligned}\left(\vec{I}+\vec{J}\right)^2 &= \begin{cases}2 & \text{triplet}\\ 0 & \text{singlet}\end{cases}\\ &= \frac{3}{2}+2\vec{I}\cdot\vec{J}\\ \vec{I}\cdot\vec{J} &= \begin{cases}\frac{1}{4} & \text{triplet}\\ -\frac{3}{4} & \text{singlet}\end{cases}.\end{aligned}$$

We denote the magnetic moments by

$$\begin{aligned}\vec{\mu}_e\cdot\vec{B} &= g_e\frac{-eB}{2m_e}J_z\equiv -k_eJ_z\\ \vec{\mu}_\mu\cdot\vec{B} &= g_\mu\frac{eB}{2m_\mu}I_z\equiv k_\mu I_z,\end{aligned} \tag{3}$$

and introduce $\delta k=\frac{k_e-k_\mu}{\Delta E_{\mathrm{HFS}}}$ and $x=\frac{k_e+k_\mu}{\Delta E_{\mathrm{HFS}}}$. With this notation the Hamiltonian (2) in the basis $|11\rangle$, $|1-1\rangle$, $|10\rangle$, $|00\rangle$ (where the first number denotes the total spin and the second is its z projection) can be written as

$$H = \frac{\Delta E_{\mathrm{HFS}}}{2}\begin{pmatrix}\frac{1}{2}+\delta k & & & \\ & \frac{1}{2}-\delta k & & \\ & & \frac{1}{2} & x\\ & & x & -\frac{3}{2}\end{pmatrix}.$$

We find the eigenvalues $\frac{1}{2}\pm\delta k$ and $-\frac{1}{2}\pm\sqrt{1+x^2}$ in units of $\Delta E_{\mathrm{HFS}}/2$.

Due to the mass difference, the electron energy in the magnetic field is much larger than the corresponding energy for the muon, $k_e\gg k_\mu$. Also, for moderate field B, $k_e\ll\Delta E_{\mathrm{HFS}}$. The difference of the two eigenvalues that grow with B is

$$\begin{aligned}\nu_{12} &= \frac{\Delta E_{\mathrm{HFS}}}{2}+\frac{k_e-k_\mu}{2}-\frac{\Delta E_{\mathrm{HFS}}}{2}\sqrt{1+x^2}\\ &= -k_\mu+\frac{\Delta E_{\mathrm{HFS}}}{2}\left(1+x-\sqrt{1+x^2}\right).\end{aligned}$$

The difference of the two remaining ones is

$$\begin{aligned}\nu_{34} &= \frac{\Delta E_{\mathrm{HFS}}}{2}-\frac{k_e-k_\mu}{2}+\frac{\Delta E_{\mathrm{HFS}}}{2}\sqrt{1+x^2}\\ &= k_\mu+\frac{\Delta E_{\mathrm{HFS}}}{2}\left(1-x+\sqrt{1+x^2}\right),\end{aligned}$$

so that

$$\begin{aligned}\nu_{12}+\nu_{34} &= \Delta E_{\mathrm{HFS}},\\ \nu_{34}-\nu_{12} &= 2k_\mu+\Delta E_{\mathrm{HFS}}\left(\sqrt{1+x^2}-x\right).\end{aligned}$$

The expressions for the transition frequencies are known as the Breit-Rabi formula [23]. In addition to ν_{12} and ν_{34}, also the Larmor frequency of the proton is measured,

$$2\mu_pB=\nu_p. \tag{4}$$

This equation allows one to eliminate the relatively poorly known B when the ratio $\frac{\mu_\mu}{\mu_p}$ is calculated from the measured frequencies.

Before this ratio is used in the measurement of the (free) muon anomalous magnetic moment we need to correct the g-factor in Eq. (3) for binding effects,

$$g_\mu\to g_\mu\left(1-\frac{\alpha^2}{3}+\frac{\alpha^2}{2}\frac{m_e}{m_\mu}+\ldots\right). \tag{5}$$

In the limit of $m_e\to 0$ the size of muonium becomes infinite, and we expect that binding corrections to the muon g-factor to vanish as the muon will be unaffected by the electron at infinity. However, the binding corrections in Eq. (5) do not vanish in the limit $m_e\to 0$. The explanation of this surprising feature is that the magnetic field is treated as a perturbation in the two-particle Hamiltonian describing the muon-electron system [24]. When the mass of the electron goes to zero and the magnetic field is kept constant, the interaction energy of the muon and the electron spins with the magnetic field surpasses the electron kinetic energy. In these circumstances the magnetic field cannot be treated as a perturbation to the two-particle Hamiltonian. This is why the limit $m_e\to 0$ is nontrivial. In practical applications, the electron kinetic energy in muonium, $m_e\alpha^2/2$, is much larger than the dipole magnetic interaction and Eq. (5) remains correct.

The magnetic field is measured using nuclear magnetic resonance (NMR), with the help of the standard H_2O probes [25]. This is done by measuring the Larmor frequency $\omega_L=\gamma_IB$, where γ_I is the gyromagnetic ratio of the nucleus used in the probe. In experiments like $g_\mu-2$, we are interested in defining the field in terms of the free proton magnetic moment $B=\omega_p/\gamma_p$. This means that we need a ratio of the γ_I to the γ_p. For spherical water sample, this ratio was measured with an accuracy of 0.014 ppm. Experiment [26] measured ratio of the proton g factor in hydrogen to the electron g factor in hydrogen. They applied binding corrections to transform measured ratio of bound g-factors to the respective ratio for the free particles. Another experiment [27] measured the ratio of the g-factor of a proton in water to the electron g-factor in hydrogen. They also applied binding corrections to convert the electron g-factor in hydrogen to the free electron magnetic moment.

We see that the binding corrections to g-factors enter in a variety of ways in the determination of the muon $g_\mu - 2$. In the next Section we discuss in more detail their role in the determination of fundamental constants.

3 Magnetic moment of a bound electron

Precise measurement of the magnetic moment of an electron bound to a nucleus has recently been used to determine the electron mass [28]. In a constant magnetic field, the electron mass m_e can be calculated from the ratio of the cyclotron frequency $\nu_{\rm cyc}$ to the precession frequency of the electron spin ν_L

$$m_e = \frac{g}{2}\frac{e}{q}\frac{\nu_{\rm cyc}}{\nu_L} m_{\rm ion}, \tag{6}$$

where q is the charge of the heavy ion with mass $m_{\rm ion}$. Apart from the electron mass, the only unknown quantity is the g-factor. It can be calculated in QED [29, 30] as an expansion in $\frac{\alpha}{\pi}$ and $Z\alpha$. The g-factor of a particle bound in a Coulomb field of a point-like nucleus with charge Z was calculated in 1928 by G. Breit [31]. In the ground state of a hydrogenlike ion, the electron g-factor equals

$$g_{\rm Breit} = \frac{2}{3}\left(1 + 2\sqrt{1-(Z\alpha)^2}\right). \tag{7}$$

This results is valid to all orders in $Z\alpha$ but it neglects radiative corrections, the finite nucleus size, and recoil corrections.

Radiative corrections to the electron g-factor of the order $\left(\frac{\alpha}{\pi}\right)^n (Z\alpha)^0$ [32–35] are the same as for the free electron, where results are currently known up to $\left(\frac{\alpha}{\pi}\right)^5$ order [36]. Corrections of type $\left(\frac{\alpha}{\pi}\right)^n (Z\alpha)^2$ are universal for $n > 0$, and were calculated by Grotch [37] (see also [38]). Analytical results were also obtained for $\left(\frac{\alpha}{\pi}\right)(Z\alpha)^4$ [29] and $\left(\frac{\alpha}{\pi}\right)^2 (Z\alpha)^4$ [30]. Higher order corrections are only known numerically for the one loop case [39–41]. Recoil corrections were calculated in [42–44].

The missing corrections of the order of $\left(\frac{\alpha}{\pi}\right)^2 (Z\alpha)^5$ are now the limiting factor preventing further improvement of the electron mass determination. Authors of [28] suggested that these unknown higher order effects can be estimated by combining measurements of the electron g-factor for carbon ($Z = 6$) and silicon ($Z = 14$). This is done by postulating that experimentally measured value of the electron g-factor is

$$g_{\rm exp}(Z) = g_{\rm th}(Z) + \left(\frac{\alpha}{\pi}\right)^2 (Z\alpha)^5 b_{50}, \tag{8}$$

where $g_{\rm th}(Z)$ contains all known contributions. The coefficient b_{50} can be determined from measurements. From (6) we obtain

$$g_{\rm exp}(Z) = 2(Z-1)\frac{m_e}{m_{\rm ion}}\Gamma({\rm ion}) \tag{9}$$

where we introduced $\Gamma = \frac{v_L}{v_{\rm cyc}}$. Writing (9) and (8) for $Z = 6$ and $Z = 14$ we obtain a system of two linear equations that can be solved for the unknown m_e and b_{50}.

For completness we summarize here all input values needed for the calculation of the electron mass [28]

$$\begin{aligned} g_{\rm th}(6) &= 2.0010415901798(47), \\ g_{\rm th}(14) &= 1.995348957931(81), \\ m_{^{12}{\rm C}^{5+}} &= 11.9972576802909(11)u, \\ m_{^{28}{\rm Si}^{13+}} &= 27.9698005945(5)u, \\ \alpha &= 0.0072973525698(24), \\ \Gamma\left(^{12}{\rm C}^{5+}\right) &= 4376.21050089(11)(7), \\ \Gamma\left(^{28}{\rm Si}^{13+}\right) &= 3912.86606499(13)(13). \end{aligned} \tag{10}$$

The last number is taken from [45], since the value given in [28] contains a misprint. The final result for the coefficient b_{50} reads

$$b_{50} = -4.0(5.1). \tag{11}$$

The higher order terms in the expansion in $Z\alpha$ may contain logarithms of $Z\alpha$. These potentially large corrections limit current accuracy of determination of the electron mass from the bound g-factor measurements.

Further progress in this area can be achieved provided that the coefficient b_{50} is calculated from QED rather than determined form experiments.

Combination of measurements for different ions with theoretical calculations will lead to improvements in determination of fundamental constants. Possibly not only the electron mass but also α can be precisely measured in bound electron g-factor experiments [17]. Such a result, combined with improved measurements of the gyromagnetic ratio of the free electron, can be used to independently test the possible New Physics contribution to muon $g-2$.

4 Muon-electron conversion and the muon decay in orbit

Bound muon decay is a decay of the muon into an electron and two neutrinos $\mu^- \to e^- \overline{\nu}_e \nu_\mu$ in the presence of a nucleus with charge Ze and mass m_N. Typically the initial muon occupies the ground energy state. The maximal electron energy E_e can almost reach the muon mass, m_μ,

$$E_{\rm max} = m_\mu + E_b - E_{\rm rec}, \tag{12}$$

where the binding energy is $E_b \simeq -m_\mu \frac{(Z\alpha)^2}{2}$ and recoil energy is $E_{\rm rec} \simeq \frac{m_\mu^2}{2m_N}$. The limiting energy $E_{\rm max}$ is larger than in the free muon decay because the muon, electron, and the nucleus can transfer some momentum among each other by exchanging Coulombic photons. The recoil energy is the kinetic energy of the nucleus at maximum momentum transfer, $\vec{q}^{\,2} = m_\mu^2$.

The high-energy part of the spectrum, $\frac{m_\mu}{2} \lesssim E_e < E_{\max}$, can be described with the help of the perturbative expansion in $Z\alpha$ [46–48],

$$\frac{m_\mu}{\Gamma_0}\frac{d\Gamma}{dE} = \sum_{ijk} B_{ijk}\Delta^i (\pi Z\alpha)^j \left(\frac{\alpha}{\pi}\right)^k, \tag{13}$$

where $\Delta = \frac{E_{\max}-E}{m_\mu}$; $\Gamma_0 = \frac{G_F^2 m_\mu^5}{192\pi^3}$ is the free-muon decay rate; and G_F is the Fermi constant [49]. Powers of $\frac{\alpha}{\pi}$ parametrize radiative corrections calculated in [47]. This expansion is possible because the momentum transfer to the nucleus in the high-energy part of the spectrum is much larger than the typical bound muon momentum $m_\mu Z\alpha$.

The leading term in the expansion cannot be calculated in the Born approximation [50], i.e. when the electron is described by a plain wave and the muon is described by a non-relativistic wave function. To obtain the leading coefficient, the first relativistic correction to the muon wave function must be taken into account. When the muon exchanges a large momentum ($\vec{q}^2 \sim m_\mu^2$) with the nucleus, the first relativistic correction can be of the same order in $Z\alpha$ as the non-relativistic term obtained as a solution to the Schrödinger equation. On the other hand, if the muon momentum is small, on the order of $m_\mu Z\alpha$, the electron must transfer a large momentum to the nucleus. This can be described as the first order perturbation due to the Coulomb potential to the electron wave function. A similar reasoning is applied in the relativistic description of the atomic photoelectric effect [51]. The amplitude describing the decay in orbit (DIO) can be graphically represented as a sum of two Feynman diagrams shown in Figure 1.

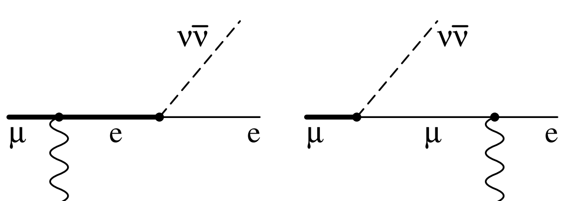

Fig. 1. Feynman diagrams representing the tree level contributions to the high-energy region of the electron spectrum in the muon decay in orbit.

When the electron energy approaches half of the muon mass, this expansion starts to diverge. This is illustrated by the red (dashed) line in Fig. 2. This divergence is a sign that the perturbative expansion breaks down, as the central region $m_\mu Z\alpha \lesssim E_e \lesssim \frac{m_\mu}{2}$ is dominated by exchanges of soft photons that transfer small amounts of momentum, typically on the order of $m_\mu Z\alpha$.

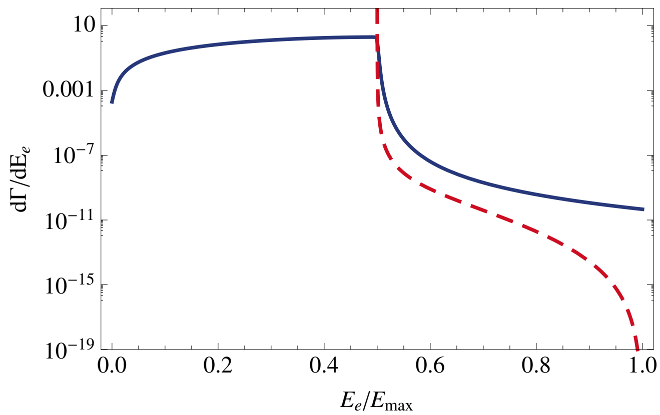

Fig. 2. Muon DIO spectrum for $Z = 1$. The red (dashed) line denotes perturbative expansion used in the high-energy region. The blue (solid) line is the spectrum obtained as a convolution of the tree level free muon spectrum convoluted with the shape function.

Before we discuss the central region of the spectrum, we mention that the radiative corrections to the term B_{550} in (13) have been recently calculated [47]. Examples of diagrams calculated in that study are shown in Figure 3.

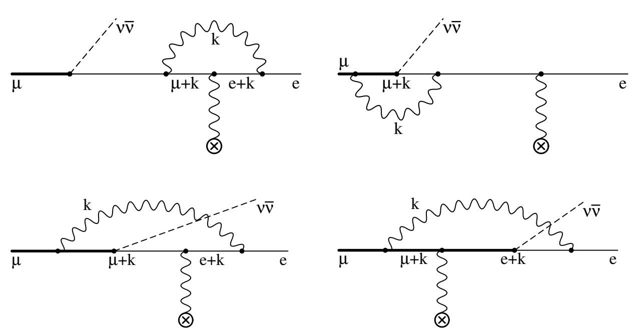

Fig. 3. Virtual corrections to the DIO spectrum near the end point (examples).

B_{550} is the leading term in the expansion around the endpoint, therefore radiative corrections are enhanced by emissions of soft and collinear photons. Soft photons generate singular factors like $\ln\Delta$; fortunately, terms containing them can be exponentiated [52]. Collinear photons produce large logarithms of the ratio of the muon and the electron masses.

Also important are the vacuum polarization corrections. In contrast to the soft and collinear photons, they increase the number of the DIO events by strengthening the Coulomb interaction at short distances. In [47] it was shown that

$$B_{550} \to B_{550}\left(\Delta^{\frac{\alpha}{\pi}\delta_{\mathrm{S}}} + \frac{\alpha}{\pi}\delta_{\mathrm{H}}\right), \tag{14}$$

where $\delta_{\mathrm{H}} = 6.31 - \frac{26}{15}\ln\frac{m_\mu}{m_e}$, and $\delta_{\mathrm{S}} = 2\ln\frac{2m_\mu}{m_e} - 2$ is a soft correction. This result is significant for experiments searching for the muon electron conversion. The signature of this exotic process is a decay of a muonic atom into a mono-energetic electron with energy $E_{\max}$, and a nucleus. A high-energy electron produced in the DIO can mimic the signal. Fortunately, the corrections (14) decrease the background by around 15% [47]. The high-energy region of the electron spectrum will be determined in the next generation of conversion searching experiments, COMET in J-PARC [53] and Mu2e in Fermilab [54].

Finally, we discuss the central region, where an accurate prediction for the DIO spectrum requires a resummation of Coulomb photons. The dominant effect that modifies the DIO spectrum in this region is the Doppler smearing due to the motion of the muon in the atom. To quantify it, we consider the ground state wave function in momentum space,

$$\psi\left(\vec{q}\right) = \frac{8\pi Z\alpha m_\mu \Psi(0)}{\left[\vec{q}^2 + (Z\alpha m_\mu)^2\right]^2}, \tag{15}$$

where $\Psi(0) = \sqrt{\frac{(Z\alpha m_\mu)^3}{\pi}}$. It can be interpreted as a momentum distribution of the muon bound to the nucleus. Muon motion in an atom can be taken into account by the shape function formalism [55, 56]. The shape function was first defined in QCD to describe heavy quarks decays [57–63]. For the muon DIO, it can be interpreted as a probability density distribution function of the muon momentum along the electron direction. As was calculated in [55],

$$S(\lambda) = \frac{8 m_\mu^5 Z^5 \alpha^5}{3\pi \left[\lambda^2 + m_\mu^2 Z^2 \alpha^2\right]^3}. \tag{16}$$

This result resembles the form of the wave function (15). The typical size of the region affected by the shape function is characterized by $\lambda \sim Z\alpha m_\mu$. The DIO spectrum is obtained as a convolution of the free muon spectrum

$$\begin{aligned} \frac{\mathrm{d}\Gamma_{\text{free}}}{\mathrm{d}x} &= \frac{G_F^2 m_\mu^5}{192\pi^3} x^2 \left(6 - 4x\right) \\ x &= \frac{2E_e}{m_\mu} \qquad 0 < x \leq 1, \end{aligned} \tag{17}$$

with the shape function (16)

$$\frac{\mathrm{d}\Gamma}{\mathrm{d}E_e} = \int \mathrm{d}\lambda\, S(\lambda) \frac{\mathrm{d}\Gamma_{\text{free}}}{\mathrm{d}z} \frac{\mathrm{d}z}{\mathrm{d}E_e}\bigg|_{z\to z(\lambda)}. \tag{18}$$

The spectrum obtained in this way is depicted in Fig. 2 with the blue (solid) line. The shape function formalism breaks down in the high-energy region because it neglects the hard Coulombic photons exchanged between the nucleus and the muon and/or the electron.

Both the leading term in the perturbative expansion and the shape function formalism describe the DIO spectrum in two separate energy region. Within the current theory, these two region do not overlap. Higher order corrections need to be calculated in order to obtain a smooth function, analytically describing the spectrum at all energies. Although such a description is available from numerical calculations [64], an analytic result will be a better basis for the determination of radiative corrections due to selfinteractions of the muon-electron line.

Acknowledgements

We thank Professor Michael Eides for a helpful discussion of the binding correction to muon magnetic moment in muonium.

References

1 T. P. Gorringe, D. W. Hertzog, Precision Muon Physics, Prog. Part. Nucl. Phys. 84 (2015) 73–123.

2 W. J. Marciano, The muon: A laboratory for 'New Physics', J. Phys. G29 (2003) 23–29.

3 Y. Kuno, Rare lepton decays, Prog. Part. Nucl. Phys. 82 (2015) 1–20.

4 J. P. Miller, E. d. Rafael, B. L. Roberts, D. Stöckinger, Muon (g-2): Experiment and Theory, Ann. Rev. Nucl. Part. Sci. 62 (2012) 237–264.

5 G. W. Bennett, et al., Final report of the muon E821 anomalous magnetic moment measurement at BNL, Phys. Rev. D73 (2006) 072003.

6 A. West. Lepton dipole moments [online] (2015). Proc. of XXXV Physics in Collision, University of Warwick [cited December 10, 2015].

7 M. Benayoun, et al., Hadronic contributions to the muon anomalous magnetic moment Workshop. $(g-2)_\mu$: Quo vadis? Workshop. Mini proceedings (2014).

8 P. Masjuan, Overview of the hadronic light-by-light contribution to the muon g-2, Nucl. Part. Phys. Proc. 260 (2015) 111–115.

9 J. Grange, et al., Muon (g-2) Technical Design Report (2015).

10 H. Iinuma, New approach to the muon g-2 and EDM experiment at J-PARC, J. Phys. Conf. Ser. 295 (2011) 012032.

11 F. Combley, F. J. M. Farley, E. Picasso, The cern muon (g-2) experiments, Phys. Rept. 68 (1981) 93.

12 H. A. Torii, et al., Precise Measurement of Muonium HFS at J-PARC MUSE, JPS Conf. Proc. 8 (2015) 025018.

13 G. Gabrielse, Measurements of the electron magnetic moment, Adv. Ser. Direct. High Energy Phys. 20 (2009) 157–194.

14 F. Biraben, Spectroscopy of atomic hydrogen, Eur. Phys. J. Special Topics 172 (2009) 109–119.

15 R. Bouchendira, P. Cladé, S. Guellati-Khélifa, F. Nez, F. Biraben, State of the art in the determination of the fine structure constant: test of Quantum Electrodynamics and determination of h/m_u, Annalen Phys. 525 (2013) 484.

16 A. Czarnecki, A Finer constant, Nature 442 (2006) 516–517.

17 V. A. Yerokhin, E. Berseneva, Z. Harman, I. I. Tupitsyn, C. H. Keitel, The g-factor of light ions for an improved determination of the fine-structure constant, arXiv:1509.08260 (2015).

18 T. Iwamoto, LFV: mu-e gamma experiment, Nucl. Part. Phys. Proc. 265-266 (2015) 320–322.

19 N. Berger, The Mu3e Experiment, Nucl. Phys. Proc. Suppl. 248-250 (2014) 35–40.

20 Y. Nakatsugawa, Search for muon to electron conversion at J-PARC MLF : Recent status on DeeMe, PoS NUFACT2014 (2015) 093.
21 D. Brown, The Mu2e Experiment: Searching for Muon to Electron Conversion, Nucl. Part. Phys. Proc. 260 (2015) 151–154.
22 P. Litchfield, COMET Phase-I, PoS NUFACT2014 (2015) 109.
23 G. Breit, I. I. Rabi, Measurement of nuclear spin, Phys. Rev. 38 (1931) 2082–2083.
24 M. I. Eides, H. Grotch, Gyromagnetic ratios of bound particles, Ann. Phys. 260 (1997) 191–200.
25 R. Prigl, U. Haeberlen, K. Jungmann, G. zu Putlitz, P. von Walter, A high precision magnetometer based on pulsed NMR, NIMA 374 (1996) 118 – 126.
26 P. F. Winkler, D. Kleppner, T. Myint, F. G. Walther, Magnetic moment of the proton in bohr magnetons, Physical Review A 5 (1972) 83.
27 W. D. Phillips, W. E. Cooke, D. Kleppner, Magnetic moment of the proton in h2o in bohr magnetons, Metrologia 13 (1977) 179.
28 S. Sturm, F. Köhler, J. Zatorski, A. Wagner, Z. Harman, G. Werth, W. Quint, C. H. Keitel, K. Blaum, High-precision measurement of the atomic mass of the electron, Nature 506 (2014) 467–470.
29 K. Pachucki, U. D. Jentschura, V. A. Yerokhin, Nonrelativistic qed approach to the bound-electron g factor, Phys. Rev. Lett. 93 (2004) 150401, erratum Phys. Rev. Lett. **94**, 229902 (2005).
30 K. Pachucki, A. Czarnecki, U. D. Jentschura, V. A. Yerokhin, Complete two-loop correction to the bound-electron g factor, Phys. Rev. A 72 (2005) 022108.
31 G. Breit, The magnetic moment of the electron, Nature 122 (1928) 649.
32 J. S. Schwinger, On Quantum electrodynamics and the magnetic moment of the electron, Phys. Rev. 73 (1948) 416–417.
33 R. Karplus, N. M. Kroll, Fourth-Order Corrections in Quantum Electrodynamics and the Magnetic Moment of the Electron, Phys. Rev. 77 (1950) 536–549.
34 A. Petermann, Fourth order magnetic moment of the electron, Helv. Phys. Acta 30 (1957) 407–408.
35 C. M. Sommerfield, Magnetic Dipole Moment of the Electron, Phys. Rev. 107 (1957) 328–329.
36 T. Aoyama, M. Hayakawa, T. Kinoshita, M. Nio, Tenth-Order QED Contribution to the Electron g-2 and an Improved Value of the Fine Structure Constant, Phys. Rev. Lett. 109 (2012) 111807.
37 H. Grotch, Electron g Factor in Hydrogenic Atoms, Phys. Rev. Lett. 24 (1970) 39–42.
38 A. Czarnecki, K. Melnikov, A. Yelkhovsky, Anomalous magnetic moment of a bound electron, Phys. Rev. A63 (2001) 012509.
39 V. A. Yerokhin, P. Indelicato, V. M. Shabaev, Evaluation of the self-energy correction to the g factor of S states in H-like ions, Phys. Rev. A69 (2004) 052503.
40 T. Beier, The g_j factor of a bound electron and the hyperfine structure splitting in hydrogenlike atoms, Phys. Rep. 339 (2000) 79.
41 R. N. Lee, A. I. Milstein, I. S. Terekhov, S. G. Karshenboim, Virtual light-by-light scattering and the g factor of a bound electron, Phys. Rev. A71 (2005) 052501.
42 V. M. Shabaev, V. A. Yerokhin, Recoil correction to the bound-electron g factor in H-like atoms to all orders in alpha Z, Phys. Rev. Lett. 88 (2002) 091801.
43 A. Yelkhovsky, Recoil correction to the magnetic moment of a bound electron, hep-ph/0108091 (2001).
44 K. Pachucki, Nuclear mass correction to the magnetic interaction of atomic systems, Phys. Rev. A78 (2008) 012504.
45 S. Sturm, A. Wagner, M. Kretzschmar, W. Quint, G. Werth, K. Blaum, g-factor measurement of hydrogenlike $^{28}\mathrm{Si}^{13+}$ as a challenge to QED calculations, Phys. Rev. A87 (2013) 030501.
46 R. Szafron, Bound Muon Decay, Acta Phys. Polon. B46 (2015) 2279.
47 R. Szafron, A. Czarnecki, High-energy electrons from the muon decay in orbit: radiative corrections, arXiv:1505.05237, Phys. Lett. B 753 (2016) 61.
48 R. Szafron, Rare muon decays, Acta Phys. Polon. B44 (2013) 2289.
49 D. Webber, et al., Measurement of the positive muon lifetime and determination of the Fermi constant to part-per-million precision, Phys. Rev. Lett. 106 (2011) 041803.
50 O. Shanker, High-energy electrons from bound-muon decay, Phys. Rev. D25 (1982) 1847.
51 V. B. Berestetsky, E. M. Lifshitz, L. P. Pitaevsky, Quantum Electrodynamics, Pergamon, Oxford, 1982.
52 D. R. Yennie, S. C. Frautschi, H. Suura, The infrared divergence phenomena and high-energy processes, Ann. Phys. 13 (1961) 379–452.
53 Y. Kuno, A search for muon-to-electron conversion at J-PARC: The COMET experiment, PTEP 2013 (2013) 022C01.
54 D. Brown, Mu2e, a coherent $\mu \to e$ conversion experiment at Fermilab, AIP Conf. Proc. 1441 (2012) 596–598.
55 R. Szafron, A. Czarnecki, Shape function in QED and bound muon decays, Phys. Rev. D92 (2015) 053004.
56 A. Czarnecki, M. Dowling, X. Garcia i Tormo, W. J. Marciano, R. Szafron, Michel decay spectrum for a muon bound to a nucleus, Phys. Rev. D90 (2014) 093002.
57 M. Neubert, Analysis of the photon spectrum in inclusive $B \to X(s)\gamma$ decays, Phys. Rev. D49 (1994) 4623.
58 M. Neubert, QCD based interpretation of the lepton spectrum in inclusive $\bar{B} \to X(u)\ell\bar{\nu}$ decays, Phys. Rev. D49 (1994) 3392.
59 I. I. Y. Bigi, M. A. Shifman, N. G. Uraltsev, A. I. Vainshtein, On the motion of heavy quarks inside hadrons: universal distributions and inclusive decays, Int. J. Mod. Phys. A9 (1994) 2467.
60 T. Mannel, M. Neubert, Resummation of nonperturbative corrections to the lepton spectrum in inclusive $B \to X\ell\bar{\nu}$ decays, Phys. Rev. D50 (1994) 2037.
61 M. Beneke, I. Z. Rothstein, M. B. Wise, Kinematic enhancement of nonperturbative corrections to quarkonium production, Phys. Lett. B408 (1997) 373–380.
62 M. Beneke, G. Schuler, S. Wolf, Quarkonium momentum distributions in photoproduction and B decay, Phys.Rev. D62 (2000) 034004.
63 C. Jin, E. A. Paschos, Radiatively corrected semileptonic spectra in B meson decays, Eur.Phys.J. C1 (1998) 523–529.
64 A. Czarnecki, X. Garcia i Tormo, W. J. Marciano, Muon decay in orbit: spectrum of high-energy electrons, Phys. Rev. D84 (2011) 013006.